

# VALIDATION OF RAIN RATE RETRIEVALS FROM SEVIRI USING WEATHER RADAR OBSERVATIONS

R. A. Roebeling and I. Holleman

Royal Netherlands Meteorological Institute (KNMI)  
P.O. Box 201, 3730 AE De Bilt, The Netherlands

## ABSTRACT

This paper presents a method to detect precipitation and estimate rain rates using cloud physical properties retrieved from the Spinning Enhanced Visible and Infrared Imager (SEVIRI). The method calculates rain rates from cloud liquid water path (*LWP*), particle effective radius, cloud thermodynamic phase and cloud top height. The accuracy of the precipitation detection and rain rate retrievals from SEVIRI is evaluated with Weather Radar observations.

Rain rates from SEVIRI are compared against Weather Radar observations for an area over Northern Europe and a two month period. The Weather Radar observations are used to validate the instantaneous rain rate retrievals and accumulated rainfall sums (precipitation depths) across the entire study area and period. In addition, we evaluate the ability of SEVIRI to discriminate precipitating from non-precipitating clouds. The results show very high agreement (corr.  $\sim 0.90$ ) between amounts of precipitating clouds detected from Weather Radar and SEVIRI observations. Although weaker correlations (corr.  $\sim 0.63$ ) are found between the rain rate retrievals from Weather Radar and SEVIRI, the SEVIRI-retrievals still have an acceptable accuracy of about  $0.2 \text{ mm hr}^{-1}$  and a precision of about  $0.7 \text{ mm hr}^{-1}$ . Part of the differences between Weather Radar and SEVIRI are explained by irregularities in the Weather Radar data due to residual sea clutter, and parallax shifts in the SEVIRI data.

In conclusion, the results of this study show the potential of SEVIRI retrieved cloud physical properties for the detection of precipitation and the retrieval of realistic rain rates. In future studies we intend to exploit the observations of the European Weather Radar network (OPERA) and extend this study to entire Europe.

## 1. INTRODUCTION

Precipitation is an important geophysical quantity that forms a crucial link between the hydrological and radiative properties of weather and climate processes. Quantitative precipitation estimates on high spatial and temporal resolutions are of increasing importance for water management and for improving parameterization cloud processes in numerical weather prediction (NWP) models or assimilation in these models. Although operational networks of Weather Radars are expanding over Europe and the United States, large areas remain where information on the occurrence of rainfall and intensity of rainfall are missing. Rain rate estimates from passive imagers operated on geostationary satellites may bridge this gap, and provide quasi-global information on the occurrence and intensity of rainfall.

Over the past decades several methods have been developed to retrieve rain rates from passive imager observations. The methods developed for geostationary satellites often use thermal infrared observations, and relate daily minimum cloud top temperatures (Adler and Negri, 1988; Anagnostou et al., 1999) or Cold Cloud Durations (CCD) to rain rates (Todd et al., 1995). The infrared based methods give fair accuracies over areas where rainfall is governed by deep convection. However, these methods perform less at higher latitudes where precipitation originates from both convective and stratiform systems. A major limitation of the CCD method is that rain rates are related to cloud duration, which is an assumption that fails in case high rain rates occur over a short period of time (Alemseged and Rientjes, 2007). More physically based are the rain rate retrieval methods that use satellite microwave radiometer (MWR) observations from instruments such as SSM/I (Wentz and Spencer, 1998). The microwave radiometer algorithms are based on the fundamental principles of radiative transfer, which use the physical relationship between MWR observed brightness temperatures and columnar water vapour and liquid water path. The rain rates are calculated the columnar liquid water path and the height of the rain column. Finally, several methods have been developed that relate rain rates to cloud physical properties retrieved from passive imagers (Rosenfeld and Gutman, 1994; Lensky and Rosenfeld, 2006; Nauss and Kokhanovsky, 2007), which use information on particle size and liquid water path to detect precipitating clouds.

Until now few studies have investigated the potential of using cloud physical property retrievals from the Spinning Enhanced Visible and Infrared Imager (SEVIRI) onboard the geostationary METEOSAT-9 to detect precipitation and derive rain rates. This paper presents the applicability of a method to detect precipitation and retrieve rain rates from SEVIRI inferred cloud microphysical properties through a comparison against Weather Radar observations. Several methods have been developed to retrieve LWP from visible and near infrared satellite radiances (Nakajima and King, 1990; King et al., 2004 and Roebeling et al., 2006). These methods retrieve Cloud Optical Thickness ( $COT$ ) and cloud droplet effective radius ( $r_e$ ) using cloud reflectances in the visible and the near infrared wavelengths, while the LWP is computed from the retrieved  $COT$  and  $r_e$ . The proposed precipitation detection and rain rate retrieval method combines the approach of Wentz and Spencer (1998) to retrieve rain rates from LWP and the height of the rain column and the approach of Rosenfeld and Gutman (1994) to detect precipitation from cloud particle effective radius and cloud thermodynamic phase. The 15 minutes sampling frequency of the METEOSAT-9 satellite allows for a statistically significant validation of rain rate retrievals from SEVIRI against Weather Radar observations.

The outline of this paper is as follows. In Section 2, the measurements of the Weather Radar and the SEVIRI instrument are described. The methods to retrieve rain rates from Weather Radar and SEVIRI observations are presented in Section 3. In Section 4, the inter-comparison procedure is described. The frequency of precipitation detection and rain rate retrievals from SEVIRI are compared against Weather Radar observations in Section 5. Finally, in Section 6, a summary is given and conclusions are drawn.

## 2. MEASUREMENTS

### *a. Weather Radar observations*

KNMI operates two identical C-band Doppler Weather Radars from Selex SI. The De Bilt radar is located at latitude  $52.10^\circ\text{N}$  and longitude  $5.18^\circ\text{E}$ . The Den Helder radar is located at latitude  $52.96^\circ\text{N}$  and longitude  $4.79^\circ\text{E}$ . The Weather Radars have recently been upgraded with digital receivers and a centralised product generation. Precipitation and wind are observed with a fourteen elevation scan (between  $0.3$  and  $25$  degrees) which is repeated every 5 minutes. From the three-dimensional scans pseudoCAPPI images, i.e., horizontal cross sections of radar reflectivity factor at constant altitude, are produced with a target height of  $1500$  m above antenna level and a horizontal resolution of  $2.4$  km (now  $1$  km). The pseudoCAPPI images from both radars are combined into the national radar composite. More details on the KNMI Weather Radar network can be found in Holleman (2005, 2007).

### *b. Satellite observations*

Meteosat Second Generation (MSG) is a European geostationary satellite that is operated by EUMETSAT. The first MSG satellite (METEOSAT-8) was launched successfully in August 2002, and positioned at an altitude of about  $36000$  km above the equator at  $3.4^\circ$  W. The SEVIRI instrument scans the complete disk of the Earth every 15 minutes, and operates three channels at visible and near infrared wavelengths between

0.6 and 1.6  $\mu\text{m}$ , eight channels at infrared wavelengths between 3.8 and 14  $\mu\text{m}$ , and one high-resolution visible channel. The nadir spatial resolution of SEVIRI is  $1 \times 1 \text{ km}^2$  for the high-resolution channel and  $3 \times 3 \text{ km}^2$  for the other channels.

### 3. METHODS

#### a. Rain rate retrieval from Weather Radar

A Weather Radar employs scattering of radio-frequency waves (5.6 GHz for C-band) to measure precipitation and other particles in the atmosphere (Rinehart, 2004). The intensity of the atmospheric echoes is converted to the so-called radar reflectivity factor  $Z$  using the Rayleigh-scattering approximation. This approximation is valid when the radar wavelength (5 cm) is much larger than the raindrop diameters ( $< 6 \text{ mm}$ ). Radar reflectivity factors are converted to rainfall intensities  $R$  using a fixed power law (Marshall and Palmer, 1948):

$$Z = 200R^{1.6} \quad (1)$$

with the radar reflectivity factor  $Z$  in  $\text{mm}^6 \text{ m}^{-3}$  and rainfall rate  $R$  in  $\text{mm h}^{-1}$ .

#### b. Rain rate retrieval from SEVIRI

The Cloud Physical Properties (CPP) algorithm of the Satellite Application Facility on Climate Monitoring (CM-SAF) is used to retrieve Cloud thermodynamic PHase ( $CPH$ ),  $COT$ , particle size and  $LWP$  from SEVIRI reflectances (Roebeling et al., 2006). The  $COT$  and particle size are retrieved for cloudy pixels in an iterative manner, by simultaneously comparing satellite observed reflectances at visible (0.6  $\mu\text{m}$ ) and near-infrared (1.6  $\mu\text{m}$ ) wavelengths to Look Up Tables (LUTs) of simulated reflectances for given optical thicknesses, particle sizes and surface albedos for water and ice clouds. These LUTs are generated with the Doubling Adding KNMI (DAK) radiative transfer model (De Haan et al., 1987; Stammes, 2001). The optical thicknesses range from 1 to 256. The particles of water clouds are assumed to be spherical droplets with effective radii between 1 and 24  $\mu\text{m}$ . For ice clouds imperfect hexagonal ice crystals (Hess et al., 1998) are assumed with effective radii between 6 and 51  $\mu\text{m}$ . The retrieval of cloud thermodynamic phase is done simultaneously with the retrieval of  $COT$  and particle size. The phase "ice" is assigned to pixels for which the 0.6  $\mu\text{m}$  and 1.6  $\mu\text{m}$  reflectances correspond to simulated reflectances of ice clouds and the cloud top temperature is smaller than 265 K. The remaining cloudy pixels are considered to represent water clouds. When a fixed vertical profile of liquid water content is assumed, the  $LWP$  can be computed from the  $COT$  and particle size retrievals. The retrievals are limited to satellite and solar viewing zenith angle smaller than  $72^\circ$ .

The algorithm for the retrieval of rain rates  $R$  is based on the parameterization proposed by Wentz and Spencer (1998), who presented the following relationship between  $LWP$  inferred from SSM/I observations and  $R$ :

$$LWP = 180 (1 + (HR)^{0.5}) \quad (2)$$

where  $LWP$  is the liquid water path in  $\text{g m}^{-2}$ ,  $R$  the rain rate in  $\text{mm hr}^{-1}$  and  $H$  the height of the rain column in km. For our application the parameterization of Wentz and Spencer (1998) is slightly modified, and rain rate is parameterized as follows:

$$LWP = 140 (1 + (H(R - \Delta R))^{0.6}) \quad (3)$$

where  $\Delta R$  is the minimum rain rate, which is set at  $0.05 \text{ mm hr}^{-1}$ . The height of the rain column  $H$  is retrieved from the difference between the maximum Cloud Top Temperature ( $CTT$ ) in the image, which is assumed to

represent a thin water cloud, and the actual  $CTT$  of the precipitating pixel. Assuming that the vertical decrease in temperature obeys a wet adiabatic lap rate of about  $6.0 \text{ K km}^{-1}$ ,  $H$  can be derived as follows:

$$H = \frac{(CTT_{\max} - CTT_{\text{pix}})}{6.0} + \Delta H \quad (4)$$

where  $\Delta H$  is the minimum height of the rain column, which is set at 0.7 km. Note that the rain rate retrievals are limited to a maximum value of  $40 \text{ mm hr}^{-1}$ , using a simple weighting function to obtain a smooth transition between retrieved rain rates and the maximum value.

The approach to detect precipitation on  $CPH$  and particle effective radius information is based on the method proposed by Rosenfeld and Gutman (1994), while the idea to use a  $LWP$  threshold to identify precipitating clouds originates from Wentz and Spencer (1998). These cloud properties provide additional criteria to separate non-precipitating clouds with small particles, for example due to pollution, from precipitating clouds with large particles or ice crystals. A Cloud is flagged as precipitating when it is an ice cloud or water cloud with droplets that have effective radii larger than  $16 \mu\text{m}$ , and it has a  $LWP$  value larger than  $150 \text{ g m}^{-2}$ .

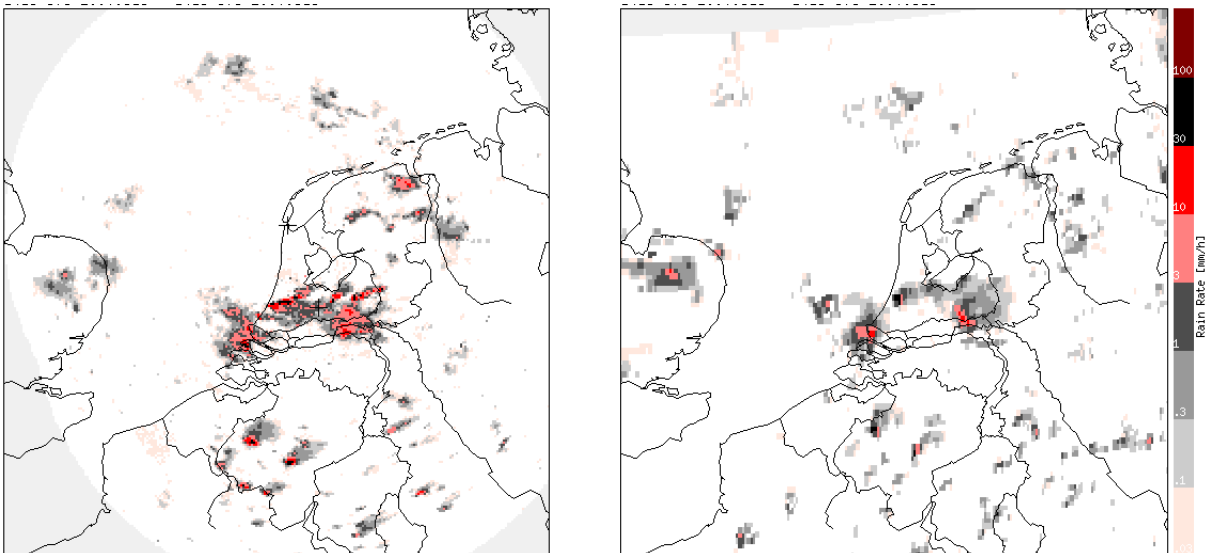
#### 4. PROCEDURE

The differences between the rain rate retrievals from Weather Radar and SEVIRI are assessed. 15 minutes SEVIRI retrievals of Cloud Physical Properties were used to generate a dataset of rain rates over North-western Europe for the summer months of May and June 2007. The reference dataset of Weather Radar data is taken from the radars of Den Helder and De Bilt in the Netherlands. In order to minimize the errors due to distance from the Weather Radar, only observation in an area of  $250 \times 250 \text{ km}^2$  are considered in our comparison study. Due to the limitation of SEVIRI to retrieve cloud properties at solar zenith angles larger than  $72^\circ$ , observation during early morning and late afternoon are excluded from the comparison. Since SEVIRI data are available at a 15 minute sampling frequency, the comparison dataset comprises about 2400 synchronized Weather Radar and SEVIRI images of rain rate.

#### 5. RESULTS

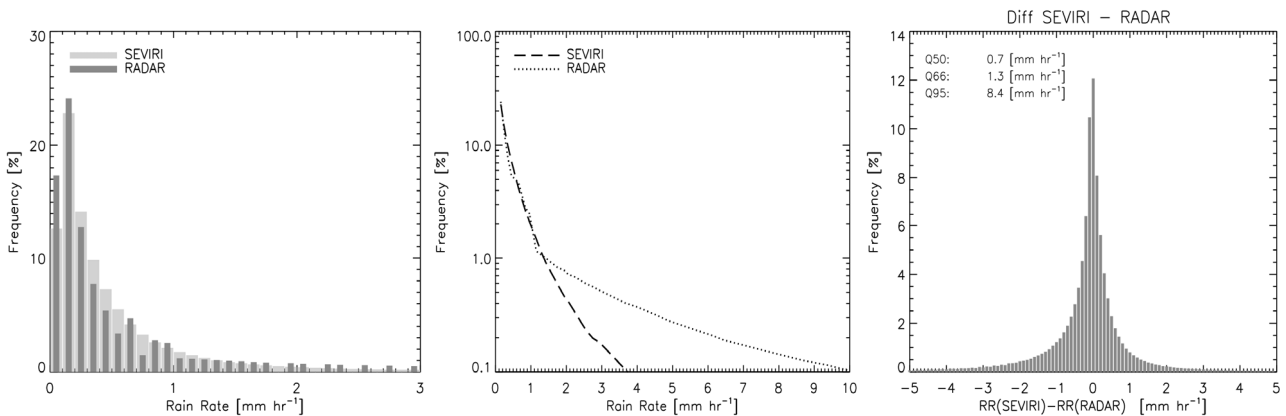
Figure 1 presents an example of rain rate retrievals from Weather Radar and SEVIRI over the study area. The images show that SEVIRI is well capable of detecting precipitating areas in the Weather Radar image. Precipitation during the selected day was characterized by convection. Visual inspection reveals that the rain rates obtained from the Weather Radar are generally higher than those from SEVIRI. However, the area and location of precipitating clouds is similar in both images. Note that the Weather Radar observations are only representative for the central part of the image, covering an area of about 150 km around the Weather radar station. Due to Earth's curvature the distance over which Weather Radars observe the entire cloud is limited to about 150 km from the ground-station (Overeem et al. 2008), whereas only the upper part of cloud is observed at longer distances, for example the precipitating clouds over Eastern United Kingdom.

Figure 2 presents the frequency distributions of rain rates retrieved from Weather Radar and SEVIRI for the study period over the Netherlands. The distributions of both instruments have similar shapes and are lognormal distributed. The right panel in the figure shows that SEVIRI observes significantly lower frequencies of precipitating clouds with rain rates larger than  $2 \text{ mm hr}^{-1}$ . This difference is partly caused by sea clutter in the rain rate observations from Weather Radar, where rain rates tend to get unrealistically high values (Holleman and Beekhuis, 2005). Another reason is that the retrieved SEVIRI cloud properties for clouds with these high rain rates are very uncertain. Roebeling et al. (2005) showed that SEVIRI cloud properties retrievals, for clouds with  $LWP$  values larger than about  $700 \text{ g m}^{-2}$ , are very sensitive to errors in cloud reflectance and radiative transfer simulations, and therefore can not be trusted. However, the



**Fig. 1. Example of rain rate retrievals from Weather Radar (left panel) and SEVIRI (right panel) at 14:15 UTC for 18 June 2007.**

frequency distribution of differences between rain rates retrieved from SEVIRI and Weather Radar (right panel in Fig. 2) reveals no systematic bias between the rain rates of both instruments. The Q50 values indicate that the SEVIRI rain rates have a precision of about  $0.7 \text{ mm hr}^{-1}$  relative to the Weather Radar retrievals. Q50 is the difference between the 25% and 75% quantiles of the deviations of the rain rate values from SEVIRI and Weather Radar, which is an alternative measure of one standard deviation. The fact that the upper and lower 25% of the dataset are ignored makes Q50 a more robust estimator of variance than the standard deviation, and the preferred one for non-Gaussian distributions.



**Fig. 2. Frequency distributions of rain rates retrieved from Weather Radar and SEVIRI for the period May and June 2007 over the Netherlands presented on a normal (left panel) and lognormal (central panel) scale. The right panel shows the frequency of differences between SEVIRI and Weather Radar.**

To evaluate regional statistics of precipitation detection and rain rates, the mean percentage of precipitation detected and the mean rain rate have been calculated for the instantaneous retrievals over The Netherlands during the study period. The results are presented in Figure 3. The upper panel in Figure 4 shows that the percentage of detected precipitation varies considerably over the observation period, with precipitation percentages varying between 0 and 60% over The Netherlands in both the Weather Radar and SEVIRI statistics. Very good agreement ( $\text{corr} \sim 0.90$ ) is found between percentages of precipitation detected by the Weather Radar and SEVIRI. Over the entire study period the percentages of precipitation detected by both instruments are similar, both about 12%. The agreement between the mean rain rates from Weather Radar and SEVIRI is significantly weaker. Although the correlation between the Weather Radar and SEVIRI retrieved rain rates is reasonable ( $\text{corr} \sim 0.63$ ), the bias between both retrievals is very small ( $\sim 0.02 \text{ mm hr}^{-1}$ ). In the SEVIRI rain rate statistics there are a number of days with significantly higher mean rain rates than the Weather Radar retrievals. As stated above these large values result from the large sensitivity of SEVIRI retrievals for clouds with LWP values larger than about  $700 \text{ g m}^{-2}$ . For these clouds the retrieved LWP values

can easily increase by 500% due to small uncertainties (~1-3%) in radiative transfer simulated reflectances or due to 3-dimensional cloud effects (Roebeling et al. 2006). These sensitivities are largest during early morning or late afternoon observation times. At these times the rain rate retrievals from SEVIRI occasionally saturate and reach their maximum value of 40 mm hr<sup>-1</sup>.

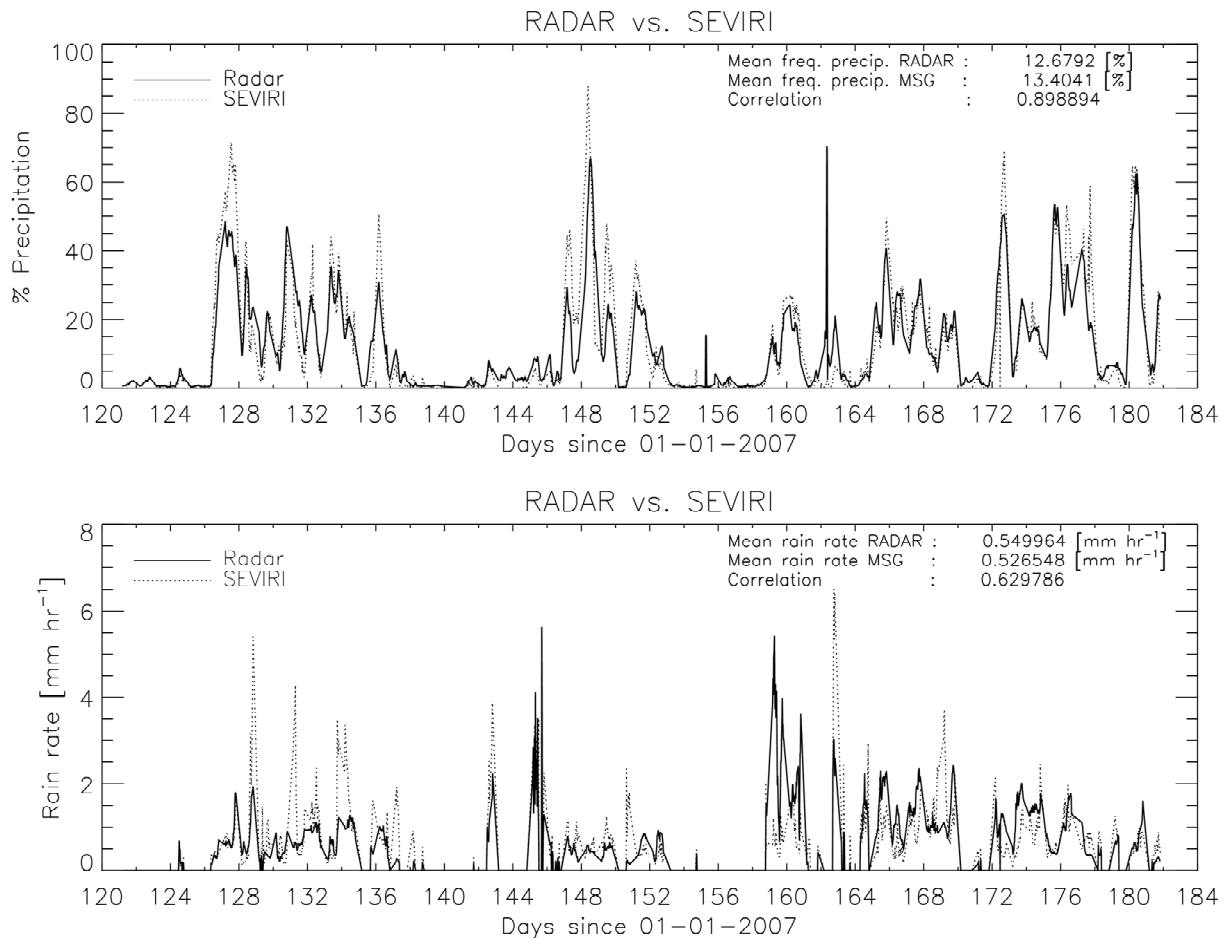


**Fig. 3. Mean percentage of precipitation and mean rain rate retrieved from Weather Radar and SEVIRI. The means are calculated over the Netherlands during the period May till June 2007.**

In Figure 4 we present images of accumulated precipitation, hereinafter referred to as precipitation depth, over the period May and June 2007. Note that the precipitation depths were only calculated for collocated and synchronized retrievals from Weather Radar and SEVIRI, which implies that these depths only include daylight observations. Visual inspection reveals that SEVIRI depicts similar precipitations depths as Weather Radar during the observation period with depths ranging between 20 and 125 mm over The Netherlands. On average the Weather Radar observes 5 to 10% larger precipitation depths than SEVIRI. The differences are largest for some local maxima in precipitation depth that are not well depicted by SEVIRI, for example the area indicated by the red circle in the images. In general the spatial dynamics in the precipitation depths from Weather Radar and SEVIRI are similar. It is promising that areas with low and high precipitation depth are observed in the same regions. This is not very obvious and only possible if the precipitation detection and the rain rate retrievals of both instruments are in the same order of magnitude. The precipitation depth values are strongly influenced by extreme rainfall events, causing that a single rainfall event heavily impacts the precipitation depth values over the observation period.

## 6. SUMMARY AND CONCLUSIONS

This paper demonstrates, for the first time, that cloud properties retrieved from geostationary satellite observations can be used to detect precipitation, retrieve rain rates and calculate precipitation depths. The

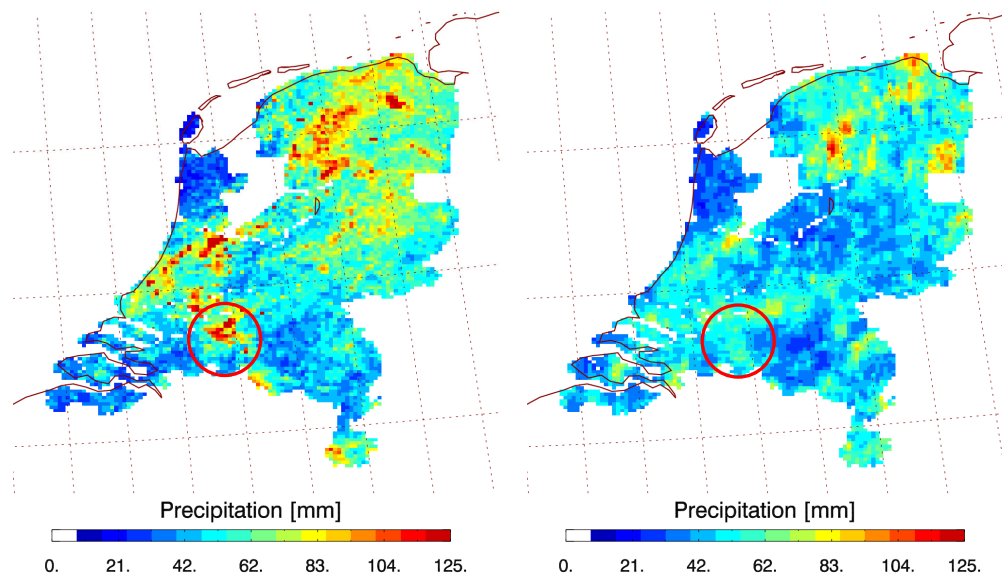


**Fig. 4. Precipitation depth in mm for May and June 2007, using collocated and synchronized retrievals from Weather Radar (left panel) and SEVIRI (right panel).**

retrieval is based on methods developed for MWR, which relate rain rates to columnar liquid water path and height of the rain column. For the detection of precipitation the clouds are analysed with respect to their liquid water path, cloud thermodynamic phase and particle effective radius. The validity of the MSG precipitation detection and rain rate retrieval methods was tested by comparing MSG retrievals against Weather Radar observations for two summer months over the Netherlands. The analysis of frequency distributions shows that SEVIRI retrieves rain rates with a high accuracy of about 2% and a satisfactory precision of about  $0.7 \text{ mm hr}^{-1}$ . SEVIRI is very accurate in detecting precipitation percentages over larger domains (The Netherlands), which is shown by correlations larger than 0.90 relative to the Weather Radar percentages. Similarly, the rain rates retrievals from SEVIRI correlate reasonably well with the Weather Radar observations (corr. = 0.63). The precipitation depths from SEVIRI and Weather Radar are similar in their mean values and spatial variations. However, the dynamics in precipitation depths are larger in the Weather Radar image than in the SEVIRI image. These differences might be due to the fact that the SEVIRI retrievals experience saturation for very thick clouds or during the unfavourable viewing conditions that occur in early morning or late afternoon. On the other hand Weather Radar retrievals saturate occasionally due to sea clutter. This study shows the potential of using SEVIRI retrieved cloud properties for precipitation detection and rain rate retrievals. Disadvantage of the proposed methods is that SEVIRI cloud properties are only retrieved during daylight hours. However, SEVIRI observations are available at a 15 minutes sampling rate for one fifth of the globe, which makes these retrievals a very valuable source of information for evaluating precipitation parameterisations in weather and climate prediction models over both land and ocean surfaces. Finally, due to including cloud phase and particle size retrievals in the precipitation detection methods, our method has the potential to study the effect of aerosols on precipitation.

## 7. ACKNOWLEDGEMENTS

This work was part of the EUMETSAT funded Climate Monitoring Satellite Application Facility (CM-SAF) project.

## 8. REFERENCES

- Adler, R. F. and A. J. Negri (1988), A satellite IR technique to estimate tropical convective and stratiform rainfall. *J. Appl. Meteorol.*, 27, 30-51.
- Alemseged, T.H. and Rientjes, T.H.M. (2007), Spatio - temporal rainfall mapping from space : setbacks and strengths. In: *Proceedings of the 5th International symposium on Spatial Data Quality SDQ 2007, Modelling qualities in space and time*, ITC, Enschede, The Netherlands, 13-15 June, 2007. Enschede : ITC, 2007. 9 p.

- Anagnostou, E. N., A. J. Negri, and R. F. Adler (1999), A satellite infrared technique for diurnal rainfall variability studies. *J. Geophys. Res.*, 104, 31477–31488.
- De Haan, J. F., P. Bosma, and J. W. Hovenier (1987), The adding method for multiple scattering calculations of polarized light, *Astron. Astrophys.*, 183, 371-391.
- Hess, M., R.B.A. Koelemeijer, and P. Stammes (1998), Scattering matrices of imperfect hexagonal ice crystals, *J. Quant. Spectros. Radiative Transfer*, 60, 301-308.
- Holleman, I. and H. Beekhuis (2005), Review of the KNMI clutter removal scheme. Technical report TR-284, KNMI, De Bilt, available via [http://www.knmi.nl/publications/fulltexts/tr\\_clutter.pdf](http://www.knmi.nl/publications/fulltexts/tr_clutter.pdf).
- Holleman, I. (2005), Quality control and verification of weather radar wind profiles, *J. Atmos. Ocean. Technol.*, 22, 1541-1550.
- Holleman, I. (2007), Bias adjustment and long-term verification of radar-based precipitation estimates, *Meteor. Appl.*, 14, 195-203.
- King, M. D., S. Platnick, P. Yang, G. T. Arnold, M. A. Gray, and J. C. Riédi, S. A. Ackerman, and K. N. Liou (2004), Remote sensing of liquid water and ice cloud optical thickness, and effective radius in the arctic: Application of airborne multispectral MAS data, *J. Atmos. Oceanic Technol.*, 21, 857-875.
- Marshall, J. S., and W. M. Palmer (1948), The distribution of raindrops with size, *J. Atmos. Sci.*, 5, 165-166.
- Nakajima, T., and M. D. King (1990), Determination of the optical thickness and effective particle radius of clouds from reflected solar radiation measurements. Part I. Theory. *J. Atmos. Sci.*, 47, 1878 – 1893.
- Overeem, A., I. Holleman, A. Buishand, Derivation of a 10-year radar-based climatology of Rainfall, *J. Appl. Meteorol. and Climatol.*, (submitted).
- Rinehart, R. E. (2004), *Radar for meteorologists*. 4th ed., Rinehart Publications, 482 pp.
- Roebeling, R.A., A. Berk, A.J. Feijt, W. Frerichs, D. Jolivet, A. Macke and P. Stammes (2005). Sensitivity of cloud property retrievals to differences in narrow band radiative transfer simulations, KNMI publication: WR-2005-02.
- Roebeling, R.A., A.J. Feijt, and P. Stammes (2006), Cloud property retrievals for climate monitoring: implications of differences between SEVIRI on METEOSAT-8 and AVHRR on NOAA-17, *J. Geophys. Res.*, 11 (D20210), doi:10.1029/2005JD006990.
- Roebeling, R.A., H.M. Deneke, and A.J. Feijt (2008), Validation of cloud liquid water path retrievals from SEVIRI using one year of CloudNET observations, *J. Appl. Meteor. Climatol.*, 47, 1, 206 – 222.
- Rosenfeld, D., G. Gutman, 1994: Retrieving microphysical properties near the tops of potential rain clouds by multispectral analysis of AVHRR data. *Atmospheric Research*, 34, 259-283.
- Stammes, P. (2001), Spectral radiance modeling in the UV-Visible range. *IRS 2000: Current problems in Atmospheric Radiation*, edited by W.L. Smith and Y.M. Timofeyev, pp 385-388, A. Deepak Publ., Hampton, Va.
- Todd, M. C., E. C. Barrett, M. J. Beaumont, and J. L. Green (1995), Satellite identification of rain days over the upper Nile river basin using an optimum infrared rain/no-rain threshold temperature model. *J. Appl. Meteorol.*, 34, 2600-2611.
- Wentz, F. J. and R. W. Spencer (1998), SSM/I Rain retrievals within a unified all-weather ocean algorithm, *J. Atmos. Sci.*, 55, 1613-1627.